14th IEA Heat Pump Conference
15-18 May 2023, Chicago, Illinois

Single Fault Impact Analysis of a Residential Heat Pump in the Cooling Mode According to the Temperature Conditions

Minkyu Jung[1], Sanghun Jeong[1], Soyeon Kim[1], Donik Ku[1], Minsung Kim[1,2*]

[1]Department of Intelligent Energy and Industry, Chung-Ang University, 84 Heukseok-ro Dongjak-gu, Seoul 06974, Republic of Korea
[2]Department of Energy Systems Engineering, Chung-Ang University, 84 Heukseok-ro Dongjak-gu, Seoul 06974, Republic of Korea

Abstract

Various faults in components of the refrigeration cycle impact on system efficiency degradation differently. In addition, since sensitive features of each fault are different, the severity of the failures varies according to the operating conditions. Therefore, impacts of residential heat pump faults according to different indoor/outdoor air conditions were analyzed. The test was implemented with R410A residential unitary split heat pump with thermostatic expansion valve (TXV). Six types of common faults were imposed individually: compressor leakage, condenser fouling, evaporator fouling, liquid line restriction, refrigerant undercharge, refrigerant overcharge. Performance parameter model using 2nd order multivariate polynomial was built based on no-fault data. The rate of performance degradation according to the change in operating conditions and the change of fault level was calculated, and the effects of each fault were analyzed. For instance, in case of the temperature difference between indoor and outdoor is small, the refrigerant flow rate increases to handle the cooling load, resulting in a steep decrease in performance at condenser fouling. On the other hand, in this case, the required evaporator capacity was reduced, so the effect of evaporator fouling was small.

Keywords: Heat Pump, Fault detection and diagnosis, Thermal expansion valve, Refrigeration cycle, Performance analysis;

1. Introduction

Demand for the air conditioning rapidly grows recently, and it results in increased energy consumption and the CO2 emissions. In the residential and the commercial building, the heating, ventilating and air conditioning (HVAC) system is the significant source of the energy consumption [1]. According to the OECD/IEA 2018, annual sales of the air conditioners increased about four times from that of 1990. [2] The fault occurrence is one of the main reasons of the energy loss in the HVAC system. And also, such inadequate handling of these problems such as degraded functioning of the components or faulty installation could affect the performance of the system substantially [3]. Fault detection and diagnosis (FDD) of the refrigeration systems is one of key methods to maintain and improve the performance [4].

Recent fault studies for the refrigeration system were focused on improving the accuracy of FDD. Rossi et al. [5] applied the Bayesian classification for the fault detection of rooftop air conditioner operation. Kim et al. [6] proposed the rule-based classifier for the residential heat pump cooling mode, with methodology for boundary direction selection. After 2010s, many studies suggested the application of artificial neural network (ANN) in HVAC systems [7-9].

However, studies about the fault impact on the HVAC system performance have been presented less. Kim et al. [10] selected the seven common faults of heat pump in cooling mode, and conducted the experiments with those faults imposed. Performance change by the single fault level was analyzed by comparing the performance parameters of the no-fault and the fault condition. Later, Kim et al. [11] compared the severity of each fault by comparing the fault levels that degrades 5% of energy efficiency ratio (EER). From the result, since the faults such as evaporator fouling fault (EF) or refrigerant overcharge fault (OC) impacts on the system performance less than other faults, so the fault has to be treated differently in real maintenance situations. Moreover, since the indoor and outdoor temperature conditions are the main parameters in heat pump system, the performance also varies with the operating conditions.

* Corresponding author. *E-mail address:* minsungk@cau.ac.kr

In this study, 40 cases of no-fault steady state experiments and 4 cases of fault tests(combination of indoor temperature conditions of 21.1 and 26.7 °C and outdoor temperature conditions of 27.8 and 37.8 °C) by Kim et al. [10] were analyzed, and the change in system performance of six single faults were observed. Six types of common faults were imposed individually: compressor leakage, condenser fouling, evaporator fouling, liquid line restriction, refrigerant undercharge, refrigerant overcharge. Each performance change at each fault implementation was analyzed using the comparison with the estimated fault-free steady-state reference value.

2. Experimental setup

2.1. System description and fault implementation

The system under the test is R410A 8.8 kW (2.5 ton) residential heat pump system with seasonal energy efficiency ratio (SEER) of 13 [12]. Fig. 1 shows the schematic diagram and the measuring parameters of the system. Constant-speed compressor and a thermostatic expansion valve (TXV) was coupled with indoor and outdoor section heat exchanger units. Detailed information of the test setup and the uncertainties of the measurement can be found in Kim et al. [10].

Six types of common faults in heat pump system and the determination of the artificial fault levels are illustrated on Table 1 [10]. Compressor leakage fault, or the valve leakage fault, was simulated by implementing a hot gas bypass line from the compressor discharge line to the suction line. Condenser fault, which implies improper outdoor air flowrate, was simulated by blocking the finned-heat exchange area. Evaporator fault was imposed by reducing the speed of the nozzle chamber fan at the end of the evaporator duct. Liquid line restriction, which is commonly occur by the pipe clogging, was mocked by controlling the pressure drop between the condenser exit and the evaporator inlet with the metering valve. Refrigerant overcharge and the undercharge were set by controlling the charge level of the system.

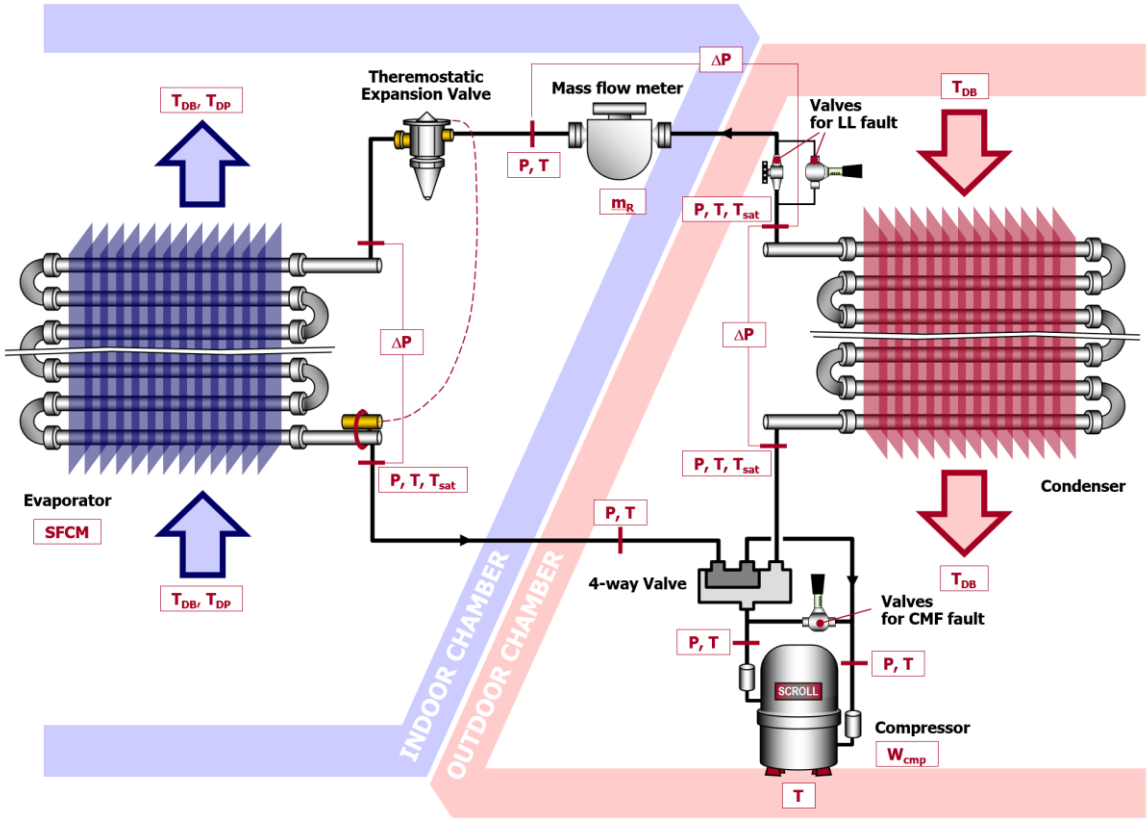

Fig. 1. Schematic diagram of cooling mode heat pump system [10].

Table 1. Description of artificial faults

Abbr.	Fault	Determination of level of artificial faults
CMF	Compressor leakage (4-way valve leakage)	% of refrigerant flow rate
CF	Improper outdoor air flow rate	% of coil area blocked
EF	Improper indoor air flow rate	% of correct air flow rate
LL	Liquid line restriction	% of normal pressure drop through TXV
OC	Refrigerant overcharge	% overcharge from the correct charge
UC	Refrigerant undercharge	% undercharge from the correct charge

2.2. Test conditions

Many studies have been analyzed the impacts of the faults in residential heat pump system, however, indoor and the outdoor temperature was seldom changed since the number of the case becomes large [10, 11, 14, 15, 16]. In order to verify the fault impact in different temperature conditions, experimental data from the Kim's study [10] was adopted. Heat pump system with six kind of single fault was tested under various conditions: indoor temperatures of 21.1, 26.7℃ and outdoor temperatures of 27.8 and 37.8℃. And each faults was tested with various fault levels: CMF (3, 6%), CF (10, 20, 35%), EF (10, 20, 30%), LL (100, 200, 300%), OC (10, 20, 30%), UC (10, 20, 30%).

3. Experimental results

3.1. Performance parameter normalization

Evaporator capacity ($\dot{Q}_{EA}$), condenser capacity ($\dot{Q}_{CA}$) and the coefficient of performance (COP) were selected as performance parameters. Since it is hard to measure the capacities when the refrigerant flows at two-phase state in faulty situations, capacities of the heat exchangers were calculated at air-side. Evaporator air-side capacity was calculated as follows:

$$\dot{Q}_{EA} = \dot{Q}_{EA,sens} + \dot{Q}_{EA,lat} \tag{1}$$

where the $\dot{Q}_{EA,sens}$ and the $\dot{Q}_{EA,lat}$ are the indoor air sensible capacity and the indoor air latent capacity, respectively. Since the measurement of the air flowrate at condenser is hard, condenser air-side capacity was calculated as Eq. (2). And the calculation of the cooling COP was shown in Eq. (3)

$$\dot{Q}_{CA} = \dot{Q}_{EA} + \dot{W}_{comp} \tag{2}$$

$$COP = \frac{\dot{Q}_{EA}}{\dot{W}_{comp}+\dot{W}_{ID,fan}+\dot{W}_{c,trans}} \tag{3}$$

Fault-free steady-state (FFSS) reference model was presented in order to estimate the reference data in no-fault situation for the performance comparison. The model was developed as a form of 2nd order multivariate polynomial equation shown in Eq. (4), with the key system parameters – indoor temperature (T_{ID}), outdoor temperature (T_{OD}) and the indoor dew point temperature (T_{IDP}) [11]. Reference values of three performance parameters at no-fault situation were approximated with regression model, and the coefficients were listed on Table 2.

$$\phi_i = a_0 + a_1 T_{ID} + a_2 T_{OD} + a_3 T_{IDP} + a_4 {T_{ID}}^2 + a_5 T_{ID} T_{OD} + a_6 T_{ID} T_{IDP} + a_7 {T_{ID}}^2 + a_8 T_{OD} T_{IDP} + a_9 {T_{IDP}}^2 \tag{4}$$

Performance variation of the system under single faults were indicated with the $r(\phi)$ of the current value and the reference value with FFSS model. The actual difference of the values, $R(\phi)$ was used when the performance variation through residual ratio is vague.

$$r(\phi) = \frac{\phi_{\text{cur}} - \phi_{\text{ref}}(T_{ID}, T_{OD}, T_{IDP})}{\phi_{\text{ref}}(T_{ID}, T_{OD}, T_{IDP})} \tag{5}$$

$$R(\phi) = \phi_{\text{cur}} - \phi_{\text{ref}}(T_{ID}, T_{OD}, T_{IDP}) \tag{6}$$

Table 2. Coefficients of 2nd-order multivariate polynomial reference model for no-fault performance estimation

ϕ_i	a0	a1	a2	a3	a4	a5	a6	a7	a8	a9
COP	2.58e+1	-5.39e-1	-3.66e-2	-4.52e-3	-4.07e-3	-2.95e-4	-3.79e-4	1.08e-4	-1.97e-4	6.12e-4
$\dot{Q}_E$	2.04e+2	1.69e+2	9.80e+0	-4.73e+1	-4.28e-1	-5.24e-2	-4.17e+1	-1.87e-1	-3.58e-1	1.35e+0
$\dot{Q}_C$	-1.61e+4	6.32e+2	1.91e+0	-5.26e+1	-3.51e+0	-1.16e-1	-2.18e-1	2.99e-2	-3.47e-1	1.23e+0

3.2. Performance degradation with single fault imposed

3.2.1. CMF fault (Compressor/valve leakage)

In Fig. 2 performance parameters with temperature conditions change of CMF fault were shown. Since the COP degradation was not significant in CMF fault, the performance change was shown in $R(\phi)$. According to the Fig. 2 (a), (c), (e), performance decreases as the outdoor temperature increases. Evaporation pressure increases as the indoor temperature increases, which results in the decrease of compression ratio from 3 to 2.2, so the volumetric efficiency increases 8% [13-15]. The specific volume of the refrigerant at compressor suction side decreases 20% as the indoor temperature increases. This leads to the increase of mass flowrate at the compressor, according to the Eq. (7) [16].

$$\dot{m}_{r,comp} = \eta_v \frac{NV_S}{v_{comp,suc}} \tag{7}$$

Since the tendency of the volumetric efficiency change is larger than the specific volume change, the mass flow rate changes inversely proportional to the outdoor temperature. Therefore, the degradation of the performance was greater at the outdoor temperature change.

3.2.2. CF fault (Improper outdoor air flow rate)

According to the Fig. 3, performance degradation was little at such low fault level of 10%, and the low temperature difference at fault level of 20%. In case of largest temperature difference (T_{ID} = 21.1 ℃, T_{OD} = 37.8 ℃) at 20% fault level, the performance drop was large because of the large pressure difference between the condenser and the evaporator. Since the heat exchanger is designed with sufficiently high safety factor, so the performance drop is still tolerable in 20% fault level. But when the fault level reaches 35%, the evaporator and the condenser capacity decrease sharply, which leads in severe performance decrease even at small indoor-outdoor temperature difference.

3.2.3. EF fault (Improper indoor air flow rate)

The decrease of the evaporator air flowrate leads to the decrease of evaporating temperature. According to the Fig. 4, three performance parameter change was less than 8% regardless of the fault level. The evaporator capacity decreases as the fault level gets higher and the condenser capacity decreases similarly. Mass flow rate of the refrigerant decreases with the decreasing evaporating temperature, however the performance of the system increases when the mass flow rate compensated by the increased indoor temperature. Moreover, at high fault level, the refrigerant mass flow rate is too small, so the sufficient system performance could be obtained with little air flow.

3.2.4. LL fault (Liquid line restriction)

LL fault was determined with the pressure difference between the TXV inlet part and discharge part. The flow rate of the refrigerant passing through the evaporator decreases with the fault level increases, so the refrigerant at the rear part of the evaporator superheated, and the opening rate of the TXV increased. At the fault level of 300%, when the temperature difference is smallest, the degradation of the performance was the highest. Condensing pressure was not changed as the operating condition changes, but the evaporating pressure changes drastically. This leads the specific volume of the refrigerant at the compressor suction side increases with the indoor temperature, and the mass flowrate at the compressor gets low. So, the refrigerant flows in two-phase and the performance degradation becomes greater. LL fault shows the largest drop of performance than the other faults.

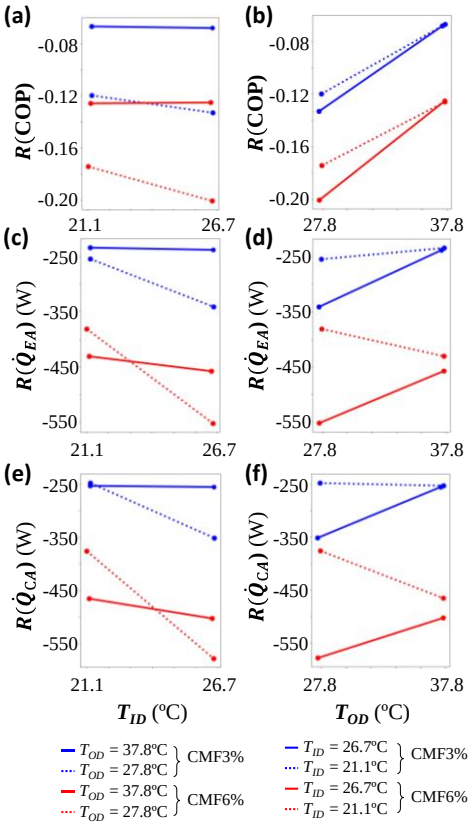

Fig. 2. Performance parameters with temperature conditions of CMF fault

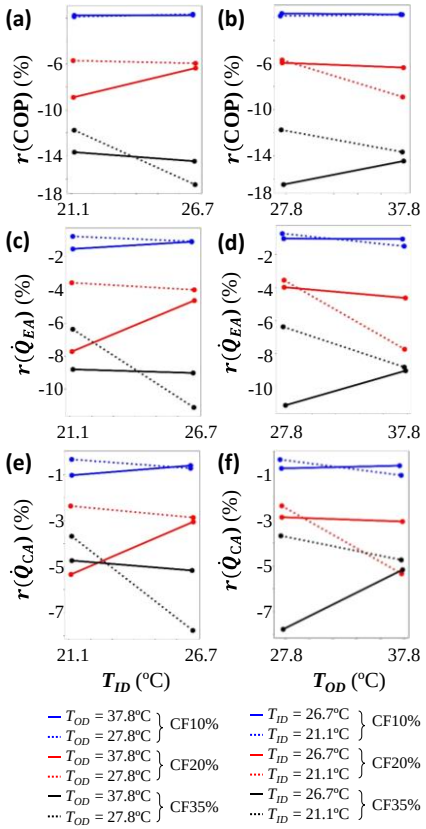

Fig. 3. Performance parameters with temperature conditions of CF fault

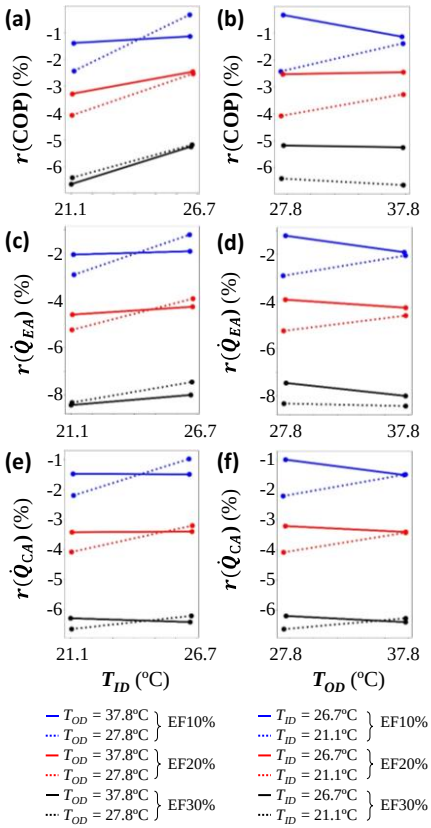

Fig. 4. Performance parameters with temperature conditions of EF fault

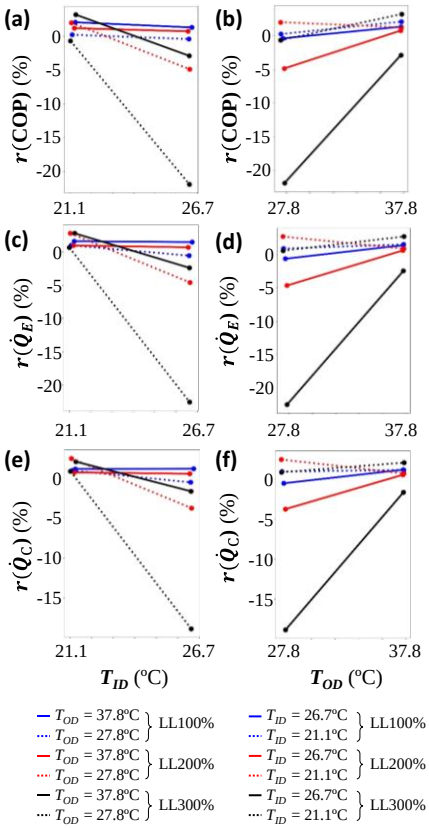

Fig. 5. Performance parameters with temperature conditions of LL fault

3.2.5. OC fault (Refrigerant overcharge)

From the Fig. 6, the system performance degrades a little, at relatively high fault level of 30%. Since the performance of the residential heat pump system is steady even if the amount of refrigerant charge is larger than the normal, performance degradation is not large when the OC fault occurs. In case of 10% fault level, at the refrigerant flowrate gets low when the indoor-outdoor temperature difference is high, the system performance was improved due to the increase of evaporation capacity. However, the OC fault could cause the inflow of liquid refrigerant in compressor, so the fault diagnosis to provide this problem is needed.

3.2.6. UC fault (Refrigerant undercharge)

System performance with the UC fault degrades drastically when the fault level exceeds 20%. As the indoor temperature increases, the mass flowrate increases due to the change of specific volume at the compressor suction side. Therefore, in high indoor temperature condition, required refrigerant is large, so the degree of superheat increased to open TXV. So, the refrigerant flows in two-phase at liquid line and the performance drop exceedingly.

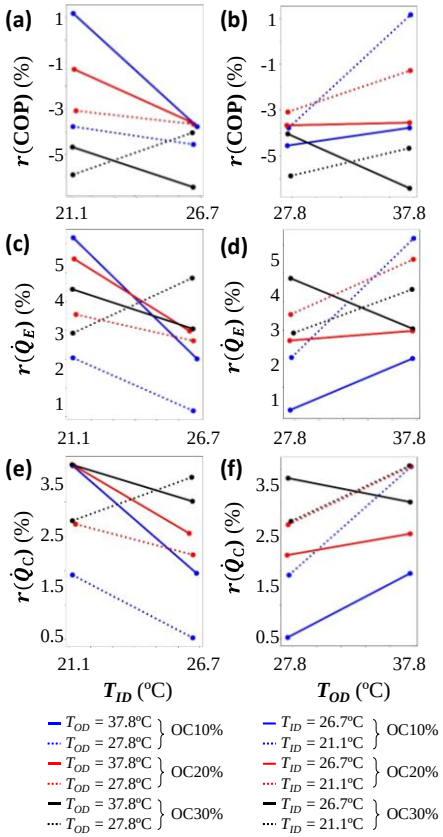

Fig. 6. Performance parameters with temperature conditions of OC fault

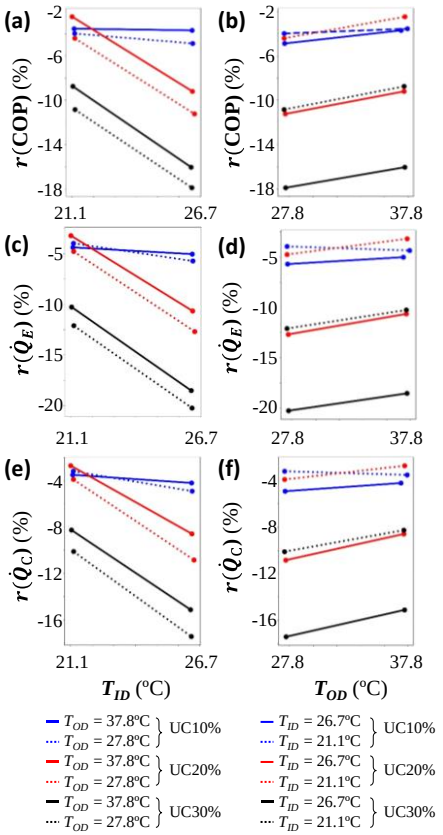

Fig. 7. Performance parameters with temperature conditions of UC fault

3.3. Comparative evaluation of fault effects in operating temperature conditions

Fig. 8 and 9 shows the COP degradation ratio at four different operating temperature conditions in mild fault level and severe fault level, respectively. As shown in Table 1, each fault level was determined in different point of view, so the first and the last fault level was selected.

According to the Fig. 8 COP degrades greatly at CMF, OC and the UC faults. The performance of the system changes intensely by the operating temperature at EF, LL and OC faults. In highest load condition (T_{ID} = 21.1 ℃, T_{OD} = 37.8 ℃), the system performance was improved at LL and OC fault. In LL fault, without lowest load condition (T_{ID} = 26.7 ℃, T_{OD} = 27.8 ℃), system performance was improved rather than the reference value.

In high fault levels, performance drop was severe of maximum 23% at LL fault. In LL fault, the effect of the fault was highlighted at lowest load condition (T_{ID} = 26.7 °C, T_{OD} = 27.8 °C). On the other hand, at highest load condition (T_{ID} = 21.1 °C, T_{OD} = 37.8 °C), system performance was improved. Accordingly, faults that affects the refrigerant mass flow rate such as LL or UC was influenced greatly by the operation temperature.

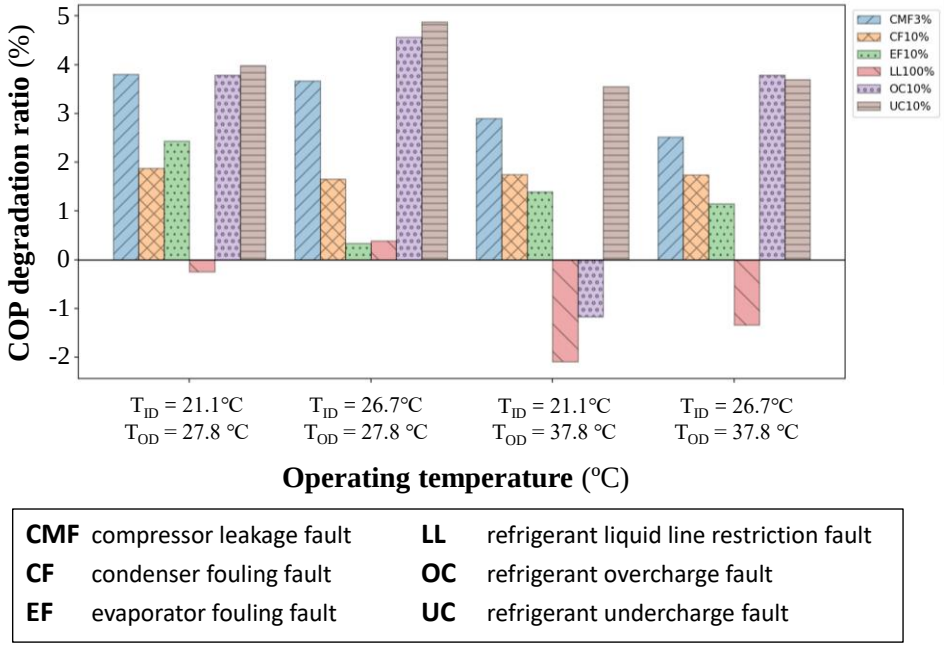

Fig. 8. COP degradation for each mild fault at four different operating temperature conditions.

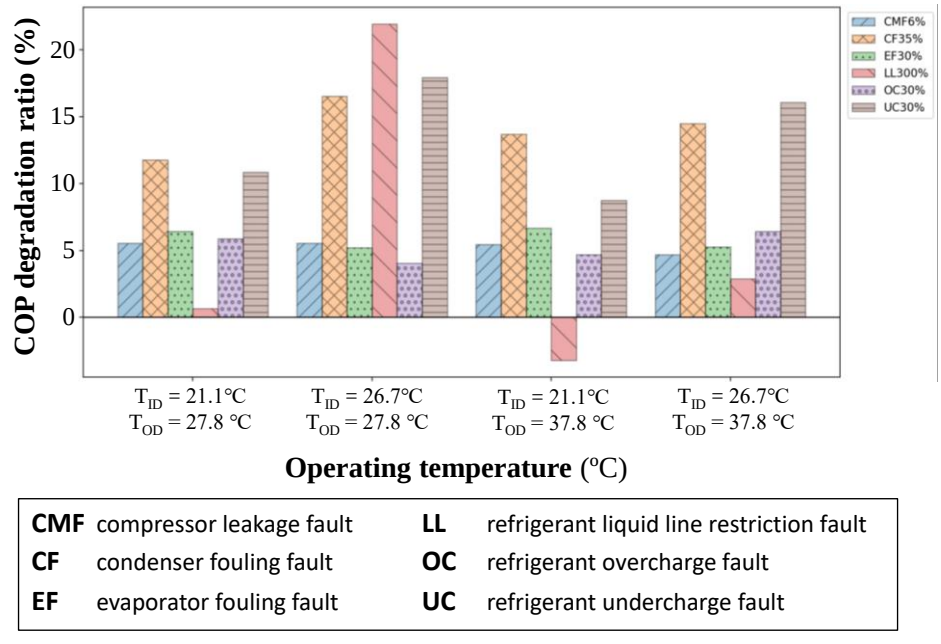

Fig. 9. COP degradation for each high fault at four different operating temperature conditions.

4. Conclusion

In this study, impact of single faults on performance of the residential heat pump system was analyzed at different operating temperature conditions. With the no-fault test data and the 2nd order multivariate

polynomial FFSS model, the reference value for the fault test was approximated. By comparing the difference between the reference value and the test data with six single faults imposed, performance difference was observed.

In CMF fault, three selected performance parameters do not fluctuate greatly, but the refrigerant flow backwards at the compressor so that the COP drops less. For CF fault, as the indoor temperature increased, the mass flowrate of the refrigerant increased, so the performance degrades less but the influence of the outdoor temperature is insignificant since the area of outdoor heat exchanger unit is decreased by the fault. At EF fault, as the evaporator air flow rate decreases, the evaporation pressure gets lower and the specific volume of the compressor suction side changes. In LL fault, as the fault level increases, the density of the fluid decreases as the evaporation temperature drops. Therefore, the refrigerant flowrate decreases greatly, and exceeds the capacity of TXV can rise. In OC fault, as charge level of the refrigerant increases the compressor work also increases which leads in COP drop. When the UC fault level gets higher, discharge line of the evaporator is superheated in order to compensate the fault by opening the TXV, which causes the two-phase flow in liquid line and the system performance reduces poorly.

Nomenclature

CF	condenser fouling	$\dot{Q}_{CA}$	condensing air-side capacity (kW)
CMF	compressor leakage	R	residual
CNN	convolutional neural network	r	residual ratio (%)
COP	coefficient of performance	ref	reference value
cur	current value	SEER	seasonal energy efficiency ratio (BTU/(W h))
DNN	deep neural network	T_{ID}	indoor temperature (℃)
DRNN	deep recurrent neural network	T_{OD}	outdoor temperature (℃)
DSH	evaporator superheat (℃)	T_{IDP}	indoor dew point temperature (℃)
EEV	electric expansion valve	TXV	thermostatic expansion valve
EF	evaporator fouling	UC	refrigerant undercharge
FDD	fault detection and diagnosis	VRF	variable refrigerant flow
FXO	fixed orifice expansion device	$\dot{W}_{c,trans}$	transformer work (kW)
HVAC	heating, ventilating, and air-conditioning	$\dot{W}_{comp}$	compressor work (kW)
LL	liquid line restriction fault	$\dot{W}_{ID,fan}$	indoor fan work (kW)
$\dot{m}_{r,comp}$	compressor mass flow rate (kg/s)		
OC	refrigerant overcharge	*Greek symbols*	
$\dot{Q}_{EA}$	evaporating capacity (kW)	ϕ	characteristic performance parameter
$\dot{Q}_{EA,lat}$	evaporating latent capacity (kW)	η_v	volumetric efficiency of compressor (%)
$\dot{Q}_{EA,sens}$	evaporating sensible capacity (kW)	$v_{comp,suc}$	compressor suction specific volume (kg/m^3)

Acknowledgements

This research was jointly supported by National Research Foundation of Korea (NRF No. 2019R1A2C108869414) and by Korea Institute of Energy Technology Evaluation and Planning (KETEP) (20202020900290, 20214000000280, 20212050100010) funded by Ministry of Trade, Industry and Energy. This research was also supported by the Korea Environmental Industry & Technology Institute (KEITI No. 2020003060005) Authors sincerely appreciate their supports.

References

[1] Afroz Z, Shafiullah GM, Urmee T, Higgins G. Modeling techniques used in building HVAC control systems: A review. *Renewable Sustainable Energy Rev.* 2018;**83**:64-84.
[2] IEA, 2018. “The Future of Cooling”. IEA, Paris, France.
[3] Mirnaghi MS, Haghighat F. Fault detection and diagnosis of large-scale HVAC systems in buildings using data-driven methods: A comprehensive review. *Energy Build.* 2020; **229**:110492.
[4] Kim W, Braun JE. Development, implementation, and evaluation of a fault detection and diagnostics system based on integrated virtual sensors and fault impact models. *Energy Build.* 2020;**228**:110368.

[5] Rossi TM, Braun JE. A statistical, rule-based fault detection and diagnostic method for vapor compression air conditioners. *HVAC&R Res.* 1997;**3**:19-37.
[6] Kim M, Yoon SH, Payne WV, Domanski PA. 2008. "Cooling mode fault detection and diagnosis method for a residential heat pump" NIST Special Publication. 1087
[7] Eom YH, Yoo JW, Hong SB, Kim MS. Refrigerant charge fault detection method of air source heat pump system using convolutional neural network for energy saving. *Energy* 2019;**187**:115877.
[8] Taheri S, Ahmadi A, Mohammadi-Ivatloo B, Asadi S. Fault detection diagnostic for HVAC systems via deep learning algorithms. *Energy Build.* 2021;**250**:111275.
[9] Wan H, Cao T, Hwang Y, Oh S. A review of recent advancements of variable refrigerant flow air-conditioning systems. *Appl. Therm. Eng.* 2020;**169**:114893.
[10] Kim M, Payne WV, Domanski PA, Hermes CJL. 2006. "Performance of a Residential Heat Pump Operating in the Cooling Mode with Single Faults Imposed" NISTIR 7350.
[11] Kim M, Payne WV, Domanski PA, Yoon SH, Hermes CJL. Performance of a Residential Heat Pump Operating in the Cooling Mode with Single Faults Imposed. *Appl. Therm. Eng.* 2009;**29**:770-8.
[12] ARI Standard, 2006. "Standard for Unitary Air Conditioning and AirSource Heat Pump Equipment". Air Conditioning and Refrigeration Institute, Fairfax, VA, p.210-240
[13] Cuevas C, Lebrun J, Lemort V, Winandy E. Characterization of a Scroll Compressor under Extended Operating Conditions. *Appl. Therm. Eng.* 2010;**30**:605-15.
[14] Picavet A, Ginies P., 2014. "Experimental Pressure-Volume diagrams of scroll compressors," International Compressor Engineering Conference. West Lafayette, USA, paper#2305.
[15] Mahfouz HAG, Hassan MNBW, Musa MN., 2004. "Analytical and Experimental Study on a Scroll Compressor," International Compressor Engineering Conference. West Lafayette, USA, paper#1648.
[16] Winandy E, Saavedra C, Lebrun J. Experimental analysis and simplified modelling of a hermetic scroll refrigeration compressor. *Appl. Therm. Eng.* 2002;**22**:107-20.